

# IMPROVED POTENCY AND SAFETY OF DNA-ENCODED ANTIBODY THERAPEUTICS THROUGH PLASMID BACKBONE AND EXPRESSION CASSETTE ENGINEERING

Giles Vermeire<sup>1</sup>, Elien De Smidt<sup>1,2</sup>, Nick Geukens<sup>2</sup>, James A. Williams<sup>3</sup>, Paul Declerck<sup>1,2</sup>,  
Kevin Hollevoet<sup>1,2</sup>

<sup>1</sup> Laboratory for Therapeutic and Diagnostic Antibodies, KU Leuven – University of  
Leuven, 3000 Leuven, Belgium

<sup>2</sup> PharmAbs, the KU Leuven Antibody Center – University of Leuven, 3000 Leuven,  
Belgium

<sup>3</sup> Nature Technology Corporation, Lincoln, NE, USA.

Correspondence should be addressed to Paul Declerck ([paul.declerck@kuleuven.be](mailto:paul.declerck@kuleuven.be)) or  
Kevin

Hollevoet ([kevin.hollevoet@kuleuven.be](mailto:kevin.hollevoet@kuleuven.be)). Address: Laboratory for Therapeutic and  
Diagnostic Antibodies, KU Leuven – Campus Gasthuisberg, O&N II Herestraat 49 box  
820, 3000 Leuven, Belgium. Phone: +3216323431.

## SHORT TITLE

Next-generation DNA-encoded antibody expression  
platform

## KEYWORDS

Antibody gene transfer, intramuscular electroporation, muscle-specific promoter,  
minimal

plasmids, DNA

engineering

## ABSTRACT

DNA-encoded delivery of antibodies presents a labor- and cost-effective alternative to conventional antibody therapeutics. This study aims to improve potency and safety of this approach by evaluating various plasmid backbones and expression cassettes. *In vitro*, antibody levels consistently improved with decreasing sizes of backbone, ranging from conventional to minimal. *In vivo*, following intramuscular electrotransfer in mice, the correlation was less consistent. While the largest conventional plasmid (10.2 kb) gave the lowest mAb levels, a regular conventional plasmid (8.6 kb) demonstrated similar levels as a minimal Nanoplasmid (6.8 kb). A reduction in size beyond a standard conventional backbone thus did not improve mAb levels *in vivo*. Cassette modifications, such as swapping antibody chain order or use of two versus a single encoding plasmid, significantly increased antibody expression *in vitro*, but failed to translate *in vivo*. Conversely, a significant improvement *in vivo* but not *in vitro* was found with a set of muscle-specific promoters, of which a newly engineered variant gave roughly 1.5- to 2-fold higher plasma antibody concentrations than the ubiquitous CAG promoter. In conclusion, despite the limited translation between *in vitro* and *in vivo*, we identified various clinically relevant improvements to our DNA-based antibody platform, both in potency and biosafety.

## INTRODUCTION

Monoclonal antibodies (mAbs) have become mainstay in a wide range of indications such as cancer and inflammatory/autoimmune disorders.<sup>1</sup> However, high treatment costs and frequent high-dose administrations limit patient accessibility. An alternative approach is antibody gene transfer, where the goal is to administer the mAb-encoding nucleotide sequence rather than the protein, allowing the patient to produce the therapeutic in a cost- and labor-effective manner for a prolonged period of time.<sup>2</sup>

Viral vectors, mRNA and plasmid DNA (pDNA) have all been applied for *in vivo* expression of antibodies, both preclinically and clinically. Each platform has its own qualities and limitations. Viral vectors exhibit an exceptional transfection efficiency, resulting in high mAb levels *in vivo* for a prolonged period of time,<sup>3</sup> but remain challenged clinically due to vector immunogenicity.<sup>4</sup> mRNA presents a quick onset of expression, providing peak mAb levels just hours after delivery.<sup>5</sup> However, expression is transient and requires repeated dosing to maintain mAb levels, thus providing minimal benefit over conventional protein delivery. pDNA as a vehicle for gene transfer is an attractive approach because of the ease of manufacturing, large payload capacity, lack of cold-chain storage requirements, and favorable biosafety profile.<sup>2</sup> To enhance cellular uptake following e.g. intramuscular injection, pDNA is typically administered *in vivo* in combination with electroporation.<sup>6</sup> The concept of DNA-encoded antibodies is currently being investigated in the clinic (NCT04079166 and NCT03831503). The momentum of this field is illustrated by the increasing support by large pharmaceutical companies and funding agencies. One notable example is the US Defense Advanced Research Projects Agency (DARPA) Pandemic Prevention Program (P3), initiated in 2017, aimed at the rapid discovery, testing, and manufacture of antibody treatments, including pDNA- or mRNA-based delivery, to fight any emerging disease threat. The P3 Program was consequently also applied in response to the COVID-19 outbreak.

Our group has previously demonstrated proof of concept for intramuscular DNA-encoded antibody gene transfer in mice and sheep. In both animal models, mAb plasma levels peak at single to double-digit  $\mu\text{g}/\text{mL}$  range two to four weeks after delivery, after which levels steadily decline but remain detectable for several months up to a year.<sup>7,8,9</sup> Comparable mAb levels have been reported in other studies.<sup>10, 11, 12</sup> Despite progress made in pre-clinical research and early clinical trials, translation of DNA-encoded antibodies to patients is subject to further improvement. First and foremost, current achievable *in vivo* mAb levels after gene transfer are relatively low, which limits the number of therapeutic mAbs applicable for this approach. Cumulative pDNA dosing, although feasible,<sup>7, 8</sup> stands in contradiction to the cost-effective alternative this strategy aims to provide. Second, current plasmids typically contain large bacterial elements, such as an origin of replication and an antibiotic selection marker. These elements give rise to safety concerns and can result in increased transgene silencing.<sup>13, 14</sup> Third, mAb expression is typically driven by potent ubiquitous promoters, which can lead to undesired expression in e.g. antigen-presenting cells, potentially triggering anti-drug-antibody (ADA) and cytotoxic T lymphocyte responses.<sup>15</sup> Fourth, plasmids that contain repeats of sequences, e.g. two identical expression cassettes for expression of the light and heavy chain, respectively, are prone to recombination and make production more challenging.<sup>16</sup>

The present study aims to address these hurdles and build towards a next-generation DNA-based platform for *in vivo* mAb expression, with a focus on improved safety and potency. Therefore, the impact of multiple DNA-engineering strategies on mAb expression were evaluated *in vitro* and *in vivo*. 4D5, the murine equivalent of trastuzumab (Herceptin®), was used as a model, allowing prolonged expression without evoking an ADA response in immune-competent mice.<sup>7</sup> First, a number of plasmid backbones with decreasing amounts of bacterial sequences were evaluated, ranging from large conventional plasmids to a minimal Nanoplasmid (npDNA).<sup>17</sup> This plasmid has a small origin of replication (R6K) and an antibiotic-independent selection marker (RNA-out), and was selected for its potential for industrial scale-up,<sup>18</sup> a necessity for clinical translation. Second, a single plasmid encoding both mAb chains, with identical or different expression cassettes, was tested

with swapped mAb heavy and light chain configurations. This single-plasmid setup was also compared to a setup with dual plasmids, each driving expression of a mAb chain (i.e. light and heavy chain, respectively). Finally, the ubiquitous CAG was compared to a set of muscle-specific promoters.

## MATERIALS AND METHODS

### *Design and production of mAb-encoding plasmid backbones*

An overview of the various constructs and plasmid backbones evaluated in this study are provided in Table 1 and Figure 1. cpDNAL is an enlarged bacterial backbone, containing F1 and ColE1 origins (1290 basepairs - bp), ampicillin and kanamycin resistance markers (1653 bp), and non-coding sequence for a total of 3937 bp. cpDNA is our previously evaluated conventional backbone,<sup>7</sup> containing a pUC origin (715 bp), ampicillin resistance marker (861 bp), and non-coding sequence for a total of 2322 bp. Both cpDNA and cpDNAL were produced in-house in *E. coli* TOP10F' strain and purified using the NucleoBond Xtra Maxi EF kit (Machery-Nagel, Düren, Germany) following the manufacturer's instructions. RNA-out Nanoplasmids (NTC9385R, Nature Technology Corporation, Lincoln, Nebraska) carry an antisense RNA element that blocks the translation of a host chromosome encoded selectable marker (SacB) permitting sucrose selection (139 bp), an R6K origin (281 bp), and non-coding sequences for a total of 512 bp. All npDNA was produced by Nature Technology Corporation following an established procedure.<sup>19</sup> Briefly, replication was performed using proprietary Plasmid+ shake culture medium containing sucrose to select for RNA-OUT Nanoplasmid vectors. Flasks were grown with shaking to saturation at 30°C with a temperature shift to 37°C to increase plasmid copy number prior to harvest. Low endotoxin npDNA was purified using Nucleobond AX 2000 or AX 10000 columns (Macherey-Nagel). For each of the evaluated constructs, purity was verified via UV spectrophotometry, and size and integrity of the constructs was validated via agarose gel electrophoresis. All constructs were formulated and stored in sterile Milli-Q H<sub>2</sub>O.

### **Cell lines and reagents**

293F cells (Freestyle 293-F suspension cells purchased from ThermoFischer Scientific, Waltham, Massachusetts in 2015) were maintained in FreeStyle 293 expression medium (ThermoFischer Scientific). Cells were cultured in T175 flasks (Sarstedt, Nümbrecht, Germany) on an orbital shaker (ThermoFischer Scientific) at 150 rpm and 8% CO<sub>2</sub> in a 37°C humidified incubator. Murine C2C12 myoblast adherent cells (purchased from ATCC, Manassas, Virginia in 2016) were maintained in DMEM F12 (ThermoFischer Scientific) supplemented with 10% heat-inactivated fetal bovine serum (FBS, ThermoFischer Scientific). Cells were cultured in T175 flasks in a 37°C humidified incubator at 5% CO<sub>2</sub>. Identity of the 293F cell line was confirmed in 2017 using short tandem repeat analysis at the Laboratory of Forensic Biomedical Sciences (Leuven, Belgium). Identity of the C2C12 cell line was confirmed in 2018 at the IDEXX Laboratories (Ludwigsburg, Germany). All cell lines were routinely tested for *Mycoplasma* contamination. Early-passages from expanded master cell stocks were used for all experiments.

### **Mice**

Gene transfer experiments were performed in 8-9 weeks old female mice with an approximate weight of 18-20 grams. BALB/c (BALB/cAnNCrI) mice were bred at the KU Leuven Animalium or purchased at Janvier (Le Genest-Saint-Isle, France) or Envigo (Horst, The Netherlands). Blood was collected via retro-orbital bleeding, processed to plasma and stored at -20°C until analysis. All animal experiments were approved by the KU Leuven Animals Ethical Committee (project P157/2017).

### **In vitro transfection assay**

293F and C2C12 transfection assays were developed to assess 4D5 production *in vitro*. For 293F, 500 000 cells were plated into 24-well plates (Costar, Sigma-Aldrich, Saint Louis, Missouri) in FreeStyle 293 expression medium. After two hours, 0.50 µg for the largest construct or equimolar amounts were transfected per well using X-tremeGENE HP DNA Transfection Reagent (Roche, Basel, Switzerland) following the manufacturer's instructions.

For C2C12, 50 000 cells were plated into 24-well plates in DMEM F12 + 10% FBS. The

next day medium was changed to DMEM F12 without FBS. After two hours, plasmid transfections were performed as described above. Four hours after transfection, each well was spiked with DMEM F12 containing horse serum (HS), resulting in a final concentration of 2% HS. As soon as 24 hours after addition of HS, myotube formation was observed, which appeared complete after 3 to 4 days. Independent of the assay, supernatant was collected six days after transfection and stored at -20°C before analysis by ELISA. Of note, the substantial differences in setup between 293F and C2C12 transfection assays do not warrant direct comparison of the resulting absolute 4D5 expression levels. Assay readout should thus be interpreted relatively within a given assay and cell type.

#### ***Intramuscular DNA electrotransfer in mice***

Intramuscular pDNA electroporation was performed in the right *tibialis anterior* muscle following a previously optimized and validated pre-clinical protocol.<sup>7</sup> Briefly, the skin was prepared using depilatory product (Veet, Reckitt Benckiser, Slough, UK), at least one day prior to pDNA injection. Intramuscular delivery sites were injected with 40 µl of 0.4 U/µl hyaluronidase from bovine testes reconstituted in sterile saline (H4272, Sigma-Aldrich), approximately one hour prior to pDNA electrotransfer. Intramuscular injections of 30 µl of pDNA, diluted in sterile MQ H<sub>2</sub>O at 2 µg/µL for the largest constructs or equimolar amounts at lower concentrations for other constructs, were immediately followed by *in situ* electroporation using the NEPA21 Electroporator (Sonidel, Dublin, Ireland) with CUY650P5 tweezer electrodes at a fixed width of 5 mm. Signa Electrode Gel (Parker Laboratories, Fairfield, New Jersey) was applied to the muscle to decrease impedance below 0.4 Ohm. Three series of four 20 ms square-wave pulses of 120 V/cm with a 50 ms interval were applied with polarity switching after two of the four pulses. Pulse delivery was verified using the NEPA21 readout.

#### ***ELISA for mAb quantification***

4D5 levels in cell culture supernatant and in plasma samples were quantitated using a previously described HER2-coated in-house ELISA.<sup>7</sup> 178

## Statistics

Statistical analyses and figure drawing were done using GraphPad Prism 8.0 (Graphpad Software, San Diego, California). Data were presented as mean + standard error of the mean (SEM). Data of two groups were compared using unpaired Student's t-test and data of three or more groups was compared using one-way ANOVA with Tukey's multiple comparison. Two-sided p-values below 0.05 were considered significant.

## RESULTS

### *Impact of plasmid backbone size*

To evaluate the impact of the plasmid backbone on mAb expression, two conventional plasmids (cpDNAL: 3.9 kb backbone, and cpDNA: 2.3 kb backbone) and a minimal plasmid (npDNA: 0.5 kb backbone) (Figure 1) were evaluated *in vitro* in C2C12 (murine myoblast) and 293F (human embryonic kidney cells) and in BALB/c mice. All backbones were compared as a single plasmid with identical CAG-driven expression cassettes for the 4D5 heavy and light chain (referred to as "CAG-HL") using equimolar amounts of DNA. Differences between the plasmids thus resided only in the bacterial elements in the backbone (Table 1 and Figure 1).

The cpDNA backbone and CAG promoter were previously selected as lead configuration, and have been extensively used for DNA-based mAb expression.<sup>7, 8, 9, 20</sup>

In both cell lines, transfection with the minimal plasmid resulted in higher 4D5 supernatant levels than with conventional plasmids (Figure 2A-B). An inverse association was observed between the size of the plasmid backbone and the resulting 4D5 levels, providing a npDNA > cpDNA > cpDNAL potency rank order. In a first *in vivo* experiment, cpDNAL-CAG-HL was compared to npDNA-CAG-HL. npDNA-CAG-HL gave significantly higher 4D5 plasma levels starting from day seven ( $p = 0.0003$ ) until the end of follow-up (Figure 2C). cpDNAL-CAG-HL yielded peak 4D5 plasma levels of  $3.2 \pm 0.9$   $\mu\text{g}/\text{mL}$ , which remained above  $0.5 \pm 0.3$   $\mu\text{g}/\text{mL}$  throughout the 20 weeks of follow-up. npDNA-CAG-HL yielded significantly higher peak 4D5 plasma levels of  $6.8 \pm 1.3$   $\mu\text{g}/\text{mL}$  ( $p < 0.0001$ ), which remained above  $1.8 \pm 0.9$   $\mu\text{g}/\text{mL}$  throughout follow-up. In a second *in vivo* experiment, cpDNA-CAG-HL was compared to npDNA-CAG-HL. At the



two week time point, npDNA-CAG-HL demonstrated a significantly higher 4D5 plasma level than cpDNA-CAG-HL ( $p = 0.03$ ). Despite this initial statistically significant difference, mAb pharmacokinetics were comparable for both plasmids for the remaining eight weeks of follow-up (Figure 2D). Overall, a limited translation between *in vitro* and *in vivo* findings was observed. The construct with the largest bacterial backbone gave the lowest mAb concentrations, both *in vitro* and *in vivo*. However, in contrast to the *in vitro* findings, the standard (smaller) bacterial backbone gave comparable antibody levels as the npDNA *in vivo*. Nevertheless, the smaller size and limited bacterial backbone of npDNA holds benefits over conventional plasmids, and it was therefore considered the lead backbone in subsequent experiments.

### ***Expression cassette configurations in single-plasmid setup***

The above described single-plasmid setup contains two expression cassettes (in tandem) with identical promoters and polyadenylation signal sequences (Table 1). Such large tandem repeats are prone to recombination and complicate production. Furthermore, identical promoters in tandem could suffer from transcriptional interference due to competition for transcription factors,<sup>21</sup> resulting in lower mAb levels. To that end, two CMV promoters, CMV1 and CMV2, as well as a  $\beta$ -globin and bovine growth hormone polyadenylation signals, respectively, were cloned in the single npDNA backbone. CMV1 contains the human T-lymphotropic virus type I (HTLV-I) R region, which is incorporated downstream of the promoter.<sup>22</sup> CMV2 contains a CMV enhancer modified to match consensus NF- $\kappa$ B sites as well as a small-intron region of minute virus of mice (Nature Technology Corporation). CMV2 is more potent than CMV1, which was more pronounced in 293F than in C2C12 (Supplemental Figure 1). This could impact the expressed mAb chain ratio and resulting mAb levels. Indeed, excess light chain was previously observed to improve mAb levels in recombinant production.<sup>23, 24</sup> To control for the difference in promoter potency, two configurations were evaluated, with each promoter driving either the light or the heavy chain, resulting in npDNA-CMV1-H-CMV2-L and npDNA-CMV1-L-CMV2-H. As reference, constructs with two identical CMV1 promoters and  $\beta$ -globin polyadenylation sequences, as well as matching cassette order, npDNA-CMV1-HL and npDNA-CMV1-LH (Table

1), were included.

In C2C12, the constructs with two CMV1 promoters were outperformed by the constructs with CMV1 and CMV2 promoters, irrespective of antibody chain configurations (HL or LH) (Figure 3A). In 293F, this was only the case for the HL configuration (Figure 3B). The latter was confirmed in an independent repeat (data not shown). The data in C2C12 could be indicative of promoter competition, while it was less obvious in 293F. Irrespectively, the improvement linked to the use of two different promoters was rather limited. Indeed, the largest improvement of 4D5 levels in both cell lines was observed from swapping the order of the chains (HL to LH) (Figure 3A-B), while maintaining the overall framework of the expression cassettes. Given the more limited effect, promoter competition between identical cassettes was not further investigated. We then compared npDNA-CMV1-L-CMV2-H and npDNA-CMV1-H-CMV2-L *in vivo*, to further investigate the impact of swapping chain order. At day seven post gene transfer, significantly higher 4D5 plasma levels were observed for npDNA-CMV1-L-CMV2-H ( $p = 0.04$ ). Thereafter, higher 4D5 levels were observed for npDNA-CMV1-H-CMV2-L, resulting in significant differences at week five ( $p = 0.0011$ ) and six ( $p = 0.0018$ ). However, the overall pharmacokinetic profiles were comparable, and considerably lower than previous findings with CAG (Figure 2C-D).<sup>7</sup> The use of the CMV promoter was therefore not further investigated. As observed in the previous section, *in vitro* data did not correlate with *in vivo* findings, again illustrating the limited predictive value of *in vitro* data. Overall, these *in vivo* data suggest no improvement in mAb levels by swapping the mAb chain configuration.

### ***Single- versus dual-plasmid setup***

Previous experiments focused on a single plasmid driving expression of both mAb chains, which is considered preferable from a development and production perspective. However, mAbs can also be expressed through co-transfection of two plasmids, each driving the expression of the heavy and light mAb chain, respectively (Figure 1). Therefore, both cpDNA and npDNA backbones were

evaluated as a single (referred to as “HL”) or dual plasmid referred to as “H/L”) (Table 1).

In vitro, the dual-plasmid setup outperformed the single-plasmid setup for both cpDNA and npDNA. However, the improvement in 4D5 concentrations was significantly higher with the minimal plasmid, both in C2C12 ( $p < 0.0001$ ) and 293F ( $p < 0.0001$ ) (Figure 4A-B). We subsequently compared npDNA and cpDNA in a dual-plasmid setup *in vivo*. In contrast to the *in vitro* data, but similar to the *in vivo* single-plasmid data (Figure 2D), npDNA demonstrated comparable mAb pharmacokinetics as cpDNA (Figure 4C). Only at the four-week time point, mAb plasma levels were significantly higher for npDNA-CAG-H/L ( $p = 0.03$ ). As observed previously, *in vitro* data did not translate *in vivo*.

### ***Muscle-specific promoters versus CAG promoter***

Additional engineering focused on various engineered muscle-specific promoters in the dual npDNA setup. Sk-CRM4 (CRM4), MCK and MCKI are all built around the muscle-specific desmin promoter (Table 1). CRM4 contains a specifically organized transcription factor binding site cluster.<sup>25</sup> MCK carries a set of muscle creatine kinase enhancer elements as well as a small-intron region of minute virus of mice (Nature Technology Corporation). MCKI is identical to MCK, but contains specific mutations that have been demonstrated to increase expression at the cost of reduced muscle-specificity.<sup>26</sup>

To rank order potency and muscle-specificity of the promoters, transfections were carried out in C2C12 and 293F. In C2C12, npDNA-CRM4-H/L, npDNA-MCK-H/L and npDNA-MCKI-H/L yielded similar 4D5 levels compared to npDNA-CAG-H/L (Figure 5A). In 293F, 4D5 levels for the different muscle-specific promoters were more variable (Figure 5B). Assuming reduced mAb supernatant levels in 293F are reflective of improved muscle-specificity, the following specificity rank order emerged: CRM4 > MCK > CAG > MCKI. Although MCKI gave a higher expression than CAG in this assay, and consequently appears less muscle-specific, expression of a reporter using these promoters in various cell lines resulted in low expression for MCKI in two non-muscle cell lines compared to CMV (Table S1, data

provided by Nature Technologies). Subsequently, all three muscle-specific promoter constructs, npDNA-CRM4-H/L, npDNA-MCK-H/L and npDNA-MCKI-H/L, were compared *in vivo*. 4D5 plasma levels peaked between 12-16 µg/mL for each of the muscle-specific constructs (Figure 5C), higher than observed in previous experiments with the CAG promoter (Figure 4D). To confirm this, npDNA-MCK-H/L, containing the least leaky newly-engineered muscle-specific promoter (Figure 5B), was compared head-to-head to npDNA-CAG-H/L. Significantly higher mAb plasma levels were observed starting from week two after gene transfer for npDNA-MCK-H/L ( $p < 0.0001$ ), which remained throughout follow-up (Figure 5D). npDNA-MCK-H/L resulted in peak 4D5 plasma levels of  $11.1 \pm 2.3$  µg/mL, which remained above  $2.9 \pm 1.0$  µg/mL throughout the eight weeks of follow up whereas npDNA-CAG-H/L resulted in peak 4D5 plasma levels of  $6.7 \pm 2.5$  µg/mL, which remained above  $1.3 \pm 0.6$  µg/mL. In contrast to the comparable promoter strength observed in C2C12 *in vitro*, *in vivo* data show that muscle-specific promoters can result in improved mAb levels over ubiquitous promoters.

## DISCUSSION

In the current study, we combined engineering at the level of the plasmid backbone and mAb expression cassette to generate a safer and more potent DNA-based platform for intramuscular antibody gene transfer. Improvements could strengthen the potential and broaden the implementation of DNA-encoded antibodies, and possibly be translated to other DNA-encoded therapeutics.

Conventional plasmids typically contain bacterial elements. Especially antibiotic resistance markers carry biological safety concerns, and regulatory authorities recommend avoiding them for therapeutic use.<sup>27, 28</sup> Thereto, plasmid backbones free of antibiotic resistance markers have been developed and validated for large-scale antibiotic-free manufacturing, such as pCOR, pORT and npDNA (NTC9385R), the format investigated in this study.<sup>17, 29, 30</sup> Other constructs with even less bacterial backbone have also been developed, e.g. minicircles. The manufacturing process thereof typically involves intramolecular recombination to separate the producer vector from the minicircle. This bottleneck can result

in a more labor- and cost-intensive production compared to formats that retain residual bacterial elements (reviewed in Alves et al.).<sup>31</sup> For Nanoplasmid production, a high yield antibiotic-free selection system was previously established,<sup>14, 18</sup> providing a clinically scalable manufacturing methodology in line with safety recommendations by regulatory agencies.<sup>27, 28</sup>

Overall, minimal plasmids not only provide safer alternatives, but have also demonstrated improved and/or sustained transgene expression over conventional plasmids in a variety of tissues, including lung, liver, kidney and heart.<sup>32, 33, 34, 35</sup> Indeed, smaller vectors can result in more effective cell transfection and are less prone to shear forces associated with delivery.<sup>32</sup>

This could support improved expression levels, which is critical to the success of plasmid-based antibody gene transfer. Up until now, minicircles are the only minimal plasmids reported for antibody gene transfer, albeit delivered through hydrodynamic tail vein injection and with mixed results in terms of expression levels (reviewed in Hollevoet et al.).<sup>2</sup> Nanoplasmids have not previously been explored in this context.

In our *in vitro* dataset, mAb levels were inversely correlated to plasmid size for each of the evaluated backbones, indicating a higher transfection efficiency for smaller backbones, which is in line with reported literature.<sup>36, 37, 38</sup> *In vivo*, only the largest conventional plasmid (10.2 kb) gave lower mAb levels, whereas the regular conventional plasmid (8.6 kb) demonstrated similar levels compared to npDNA (6.8 kb). These data demonstrate that a reduction in size beyond the standard conventional backbone does not improve mAb levels and further gain from backbone downsizing is likely limited. Furthermore, the conventional plasmid backbones resulted in mAb pharmacokinetics comparable to that of the Nanoplasmid, suggesting they do not suffer from increased transgene silencing.<sup>39</sup> As opposed to previous reports,<sup>32, 33, 34, 35</sup> our *in vivo* data show no improvement in transgene expression from a minimal plasmid. We believe this can possibly be attributed to differences in the expressed transgene, target tissue and/or transfection methodology. In fact, Andrews et al., using a

comparable intramuscular antibody gene transfer setup, demonstrated even higher mAb levels using a >2 kb larger backbone (gWiz > pVax),<sup>10</sup> suggesting that backbone-specific sequence elements and organization, rather than their size is relevant to the achievable transgene expression.<sup>34,40</sup> While the bacterial backbone is reduced in the Nanoplasmid, additional reduction of CpG motifs within the antibody expression cassette could improve transgene expression.<sup>41,42</sup> Overall, our current data suggest that minimal plasmids as such have little impact on the magnitude of *in vivo* antibody expression achieved through intramuscular electroporation, apart from providing a better biosafety profile. While other minimal plasmid configurations remain of interest,<sup>43</sup> the ability for upscale of plasmid production should be a key criterion for plasmid selection. Separation of the expression cassettes into two (conventional) plasmid backbones has previously resulted in improved mAb levels *in vivo*,<sup>9,10</sup> despite conflicting results *in vitro*.<sup>44</sup> In the current study, mAb levels *in vitro* were favored in the dual npDNA setup. *In vivo* however, dual cpDNA demonstrated similar mAb levels compared to dual npDNA, confirming that size reduction had minimal impact.

To further improve the safety of our plasmid system, we explored tissue-specific expression through muscle-specific promoters, which could lead to more stable prolonged transgene expression than ubiquitous promoters.<sup>7, 25, 45</sup> In C2C12, mAb levels were comparable between the muscle-specific promoters and CAG. All muscle-specific promoters gave similar, robust mAb expression *in vivo*. The newly-engineered variant, MCK, yielded roughly 1.5 to 2-fold higher plasma concentrations than the ubiquitous CAG promoter, again demonstrating lack of correlation with the *in vitro* data. mAb pharmacokinetics followed a comparable trend for CAG and all three muscle-specific promoters, indicating muscle-specific designs did not result in more stable transgene expression. To the best of our knowledge, this is the first report demonstrating that muscle-specific promoters can improve *in vivo* mAb expression over potent ubiquitous promoters.

Overall, we explored various routes to increase mAb expression. While this multitude of parameters could complicate comparison between assay readouts, it was clear that not all modifications were successful. Additional improvements in mAb expression may be achieved through alternative delivery methodology, including adaptations of the formulation and delivery device,<sup>10, 12, 46</sup> as well as through mAb sequence optimizations.<sup>11, 12, 44, 47</sup> Of note, throughout our experiments, improvements in mAb levels *in vitro* generally did not translate *in vivo* and vice versa. The available literature provides a mixed and complex picture. While several studies confirm this lack of *in vitro* and *in vivo* correlation (e.g. for modifications in cassette configurations and orientations or antibody sequence), other studies did show a correlation.<sup>8, 10, 11, 12</sup> To possibly elucidate the origin of the *in vitro* and *in vivo* disconnect, direct transfection of C2C12 myotubes (instead of myoblasts) might be relevant. However, in preliminary experiments, transfection efficiency in fully differentiated myotubes appeared to be very low, resulting in nearly undetectable mAb levels (data not shown). In addition, it could be relevant to explore other *in vitro* setups, e.g. alternative muscle cell types, of both mouse and human origin<sup>48, 49, 50</sup> and other means of *in vitro* transfection, including electroporation. For now, the lack of translation illustrates a need for *in vivo* evaluation to select the most potent DNA-based mAb configurations. To improve and expedite clinical translation, the most promising configurations could also be evaluated in larger animal models, e.g. sheep.<sup>8</sup>

In conclusion, we evaluated various backbone and expression cassette modifications to our DNA-based antibody platform. Even though complicated by a rather limited correspondence between *in vitro* and *in vivo* findings, these efforts provide guidance on approaches for future optimization. Indeed, we identified various clinically relevant improvements in both potency and biosafety, including the use of a scalable minimal plasmid and a potent muscle-specific promoter.

## FUNDING

This research is supported by Research Foundation - Flanders (FWO: PhD mandate 1S50617N to G.V.; research project G0E2117N to P.D. and K.H.), KU Leuven (C2 grant: C22/15/024 to P.D. and K.H.), and Flanders Innovation & Entrepreneurship (VLAIO: IWT.150743 to K.H.).

## CONFLICTS OF INTEREST

James A. Williams has commercial interests in Nature Technology Corporation (Lincoln, NE, USA). All other authors declare no conflict of interest.

## AUTHOR CONTRIBUTIONS

GV, NG, JAW, PD and KH contributed to study design. GV and EDS performed experiments.

GV, EDS, JAW, NG, PD and KH interpreted results. GV wrote the manuscript, which was reviewed and edited by PD and KH. All authors reviewed and approved the manuscript for publication.



## References

1. Lu, RM, Hwang, YC, Liu, IJ, *et al.* (2020). Development of therapeutic antibodies for the treatment of diseases. *J Biomed Sci* **27**: 1.
2. Hollevoet, K, and Declerck, PJ (2017). State of play and clinical prospects of antibody gene transfer. *J Transl Med* **15**: 131.
3. Martinez-Navio, JM, Fuchs, SP, Mendes, DE, *et al.* (2020). Long-Term Delivery of an Anti-SIV Monoclonal Antibody With AAV. *Front Immunol* **11**: 449.
4. Priddy, FH, Lewis, DJM, Gelderblom, HC, *et al.* (2019). Adeno-associated virus vectored immunoprophylaxis to prevent HIV in healthy adults: a phase 1 randomised controlled trial. *The Lancet HIV* **6**: e230-e239.
5. Thran, M, Mukherjee, J, Ponisch, M, *et al.* (2017). mRNA mediates passive vaccination against infectious agents, toxins, and tumors. *EMBO Mol Med* **9**: 1434-1447.
6. Heller, R, and Heller, LC (2015). Gene electrotransfer clinical trials. *Adv Genet* **89**: 235-262.
7. Hollevoet, K, De Smidt, E, Geukens, N, *et al.* (2018). Prolonged in vivo expression and anti-tumor response of DNA-based anti-HER2 antibodies. *Oncotarget* **9**: 13623-13636.
8. Hollevoet, K, De Vleeschauwer, S, De Smidt, E, *et al.* (2019). Bridging the Clinical Gap for DNA-based Antibody Therapy through Translational Studies in Sheep. *Hum Gene Ther.*
9. Jacobs, L, De Smidt, E, Geukens, N, *et al.* (2020). DNA-based delivery of checkpoint inhibitors in muscle and tumor enables long-term responses with distinct exposure. *Molecular Therapy*.
10. Andrews, CD, Luo, Y, Sun, M, *et al.* (2017). In Vivo Production of Monoclonal Antibodies by Gene Transfer via Electroporation Protects against Lethal Influenza and Ebola Infections. *Mol Ther Methods Clin Dev* **7**: 74-82.
11. Duperret, EK, Trautz, A, Stoltz, R, *et al.* (2018). Synthetic DNA-Encoded Monoclonal Antibody Delivery of Anti-CTLA-4 Antibodies Induces Tumor Shrinkage In Vivo. *Cancer Res* **78**: 6363-6370.
12. Patel, A, Park, DH, Davis, CW, *et al.* (2018). In Vivo Delivery of Synthetic Human DNA-Encoded Monoclonal Antibodies Protect against Ebolavirus Infection in a Mouse Model. *Cell Rep* **25**: 1982-1993 e1984.

13. Chen, ZY, He, CY, Meuse, L, *et al.* (2004). Silencing of episomal transgene expression by plasmid bacterial DNA elements in vivo. *Gene Ther* **11**: 856-864.
14. Williams, JA (2014). Improving DNA vaccine performance through vector design. *Curr Gene Ther* **14**: 170-189.
15. Weeratna, RD, Wu, T, Efler, SM, *et al.* (2001). Designing gene therapy vectors: avoiding immune responses by using tissue-specific promoters. *Gene Ther* **8**: 1872-1878.
16. Oliveira, PH, Prather, KJ, Prazeres, DM, *et al.* (2010). Analysis of DNA repeats in bacterial plasmids reveals the potential for recurrent instability events. *Applied microbiology and biotechnology* **87**: 2157-2167.
17. Williams, JA (2013). Vector Design for Improved DNA Vaccine Efficacy, Safety and Production. *Vaccines (Basel)* **1**: 225-249.
18. Luke, J, Carnes, AE, Hodgson, CP, *et al.* (2009). Improved antibiotic-free DNA vaccine vectors utilizing a novel RNA based plasmid selection system. *Vaccine* **27**: 6454-6459.
19. Williams, JA, inventor; Nature Technology Corporation, assignee. Viral and non-viral nanoplasmid vectors with improved production patent WO 2019/183248 A1. 2019 2019/03/20.
20. Vermeire, G, De Smidt, E, Casteels, P, *et al.* (2020). DNA-based delivery of anti-DR5 nanobodies improves exposure and anti-tumor efficacy over protein-based administration. *Cancer Gene Ther.*
21. Curtin, JA, Dane, AP, Swanson, A, *et al.* (2008). Bidirectional promoter interference between two widely used internal heterologous promoters in a late-generation lentiviral construct. *Gene Ther* **15**: 384-390.
22. Luke, JM, Vincent, JM, Du, SX, *et al.* (2011). Improved antibiotic-free plasmid vector design by incorporation of transient expression enhancers. *Gene Ther* **18**: 334-343.
23. Schlatter, S, Stansfield, SH, Dinnis, DM, *et al.* (2005). On the optimal ratio of heavy to light chain genes for efficient recombinant antibody production by CHO cells. *Biotechnol Prog* **21**: 122-133.
24. Ho, SC, Bardor, M, Feng, H, *et al.* (2012). IRES-mediated Tricistronic vectors for enhancing generation of high monoclonal antibody expressing CHO cell lines. *J Biotechnol* **157**: 130-139.

25. Sarcar, S, Tulalamba, W, Rincon, MY, *et al.* (2019). Next-generation muscle-directed gene therapy by in silico vector design. *Nat Commun* **10**: 492.
26. Salva, MZ, Himeda, CL, Tai, PW, *et al.* (2007). Design of tissue-specific regulatory cassettes for high-level rAAV-mediated expression in skeletal and cardiac muscle. *Mol Ther* **15**: 320-329.
27. EMA (2001). Note for Guidance on the Quality, Preclinical and Clinical Aspects of Gene Transfer Medicinal Products  
[http://www.ema.europa.eu/docs/en\\_GB/document\\_library/Scientific\\_guideline/2009/10/WC500003977.pdf](http://www.ema.europa.eu/docs/en_GB/document_library/Scientific_guideline/2009/10/WC500003977.pdf).
28. FDA (1998). Guidance for human somatic cell therapy and gene therapy.  
<http://www.fda.gov/downloads/BiologicsBloodVaccines/GuidanceComplianceRegulatoryInformation/Guidances/CellularandGeneTherapy/ucm081670.pdf>.
29. Soubrier, F, Cameron, B, Manse, B, *et al.* (1999). pCOR: a new design of plasmid vectors for nonviral gene therapy. *Gene Ther* **6**: 1482-1488.
30. Cranenburgh, RM (2013). Operator-Repressor Titration: Stable Plasmid Maintenance without Selectable Marker Genes: 7-21.
31. Alves, CPA, Prazeres, DMF, and Monteiro, GA (2021). Minicircle Biopharmaceuticals—An Overview of Purification Strategies. *Frontiers in Chemical Engineering* **2**.
32. Stenler, S, Wiklander, OP, Badal-Tejedor, M, *et al.* (2014). Micro-minicircle Gene Therapy: Implications of Size on Fermentation, Complexation, Shearing Resistance, and Expression. *Mol Ther Nucleic Acids* **2**: e140.
33. Gracey Maniar, LE, Maniar, JM, Chen, ZY, *et al.* (2013). Minicircle DNA vectors achieve sustained expression reflected by active chromatin and transcriptional level. *Mol Ther* **21**: 131-138.
34. Lu, J, Zhang, F, and Kay, MA (2013). A mini-intronic plasmid (MIP): a novel robust transgene expression vector in vivo and in vitro. *Mol Ther* **21**: 954-963.
35. Schakowski, F, Gorschlüter, M, Buttgerit, P, *et al.* (2007). Minimal size MIDGE vectors improve transgene expression in vivo. *In vivo (Athens, Greece)* **21**: 17-23.
36. Bozza, M, Green, EW, Espinet, E, *et al.* (2020). Novel Non-integrating DNA Nano-S/MAR Vectors Restore Gene Function in Isogenic Patient-Derived Pancreatic Tumor Models. *Mol Ther Methods Clin Dev* **17**: 957-968.

37. Darquet, AM, Cameron, B, Wils, P, *et al.* (1997). A new DNA vehicle for nonviral gene delivery: supercoiled minicircle. *Gene Ther* **4**: 1341-1349.
38. Suschak, JJ, Dupuy, LC, Shoemaker, CJ, *et al.* (2020). Nanoplasmid Vectors Coexpressing Innate Immune Agonists Enhance DNA Vaccines for Venezuelan Equine Encephalitis Virus and Ebola Virus. *Mol Ther Methods Clin Dev* **17**: 810-821.
39. Wong, SP, Argyros, O, and Harbottle, RP (2015). Sustained expression from DNA vectors. *Adv Genet* **89**: 113-152.
40. Lu, J, Williams, JA, Luke, J, *et al.* (2017). A 5' Noncoding Exon Containing Engineered Intron Enhances Transgene Expression from Recombinant AAV Vectors in vivo. *Hum Gene Ther* **28**: 125-134.
41. Takahashi, Y, Nishikawa, M, and Takakura, Y (2012). Development of safe and effective nonviral gene therapy by eliminating CpG motifs from plasmid DNA vector. *Frontiers in bioscience (Scholar edition)* **4**: 133-141.
42. Simcikova, M, Prather, KL, Prazeres, DM, *et al.* (2015). Towards effective non-viral gene delivery vector. *Biotechnol Genet Eng Rev* **31**: 82-107.
43. Vandermeulen, G, Marie, C, Scherman, D, *et al.* (2011). New generation of plasmid backbones devoid of antibiotic resistance marker for gene therapy trials. *Mol Ther* **19**: 1942-1949.
44. Flingai, S, Plummer, EM, Patel, A, *et al.* (2015). Protection against dengue disease by synthetic nucleic acid antibody prophylaxis/immunotherapy. *Sci Rep* **5**: 12616.
45. Takeshita, F, Takase, K, Tozuka, M, *et al.* (2007). Muscle creatine kinase/SV40 hybrid promoter for muscle-targeted long-term transgene expression. *International journal of molecular medicine* **19**: 309-315.
46. N., SN, Jacklyn, N, S., YB, *et al.* (2019). Active Immunoprophylaxis and Vaccine Augmentations Mediated by a Novel Plasmid DNA Formulation. *Human Gene Therapy* **30**: 523-533.
47. Muthumani, K, Flingai, S, Wise, M, *et al.* (2013). Optimized and enhanced DNA plasmid vector based in vivo construction of a neutralizing anti-HIV-1 envelope glycoprotein Fab. *Hum Vaccin Immunother* **9**: 2253-2262.
48. Ohnota, H, Nakazawa, H, Hayashi, M, *et al.* (2020). Skeletal muscle cells derived from mouse skin cultures. *Biochemical and Biophysical Research Communications* **528**: 398-403.

49. Musarò, A, and Carosio, S (2017). Isolation and Culture of Satellite Cells from Mouse Skeletal Muscle. *Methods Mol Biol* **1553**: 155-167.

50. Owens, J, Moreira, K, and Bain, G (2013). Characterization of primary human skeletal muscle cells from multiple commercial sources. *In vitro cellular & developmental biology Animal* **49**: 695-705.

## TABLES

Table 1. Overview of key parameters of the constructs in this study

#	Single plasmid	Dual plasmids	Backbone	Enhancer	Base promoter	polyA	Size (bp)
1	<b>cpDNAL-CAG-HL</b>		cpDNAL	CMV	CAG	TK	10272
2	<b>cpDNA-CAG-HL</b>		cpDNA	CMV	CAG	TK	8662
3	cpDNA-CAG-H	<b>pDNA-CAG-H/L</b>	cpDNA	CMV	CAG	TK	5833
4	cpDNA-CAG-L		cpDNA	CMV	CAG	TK	5146
5	npDNA-CAG-H	<b>npDNA-CAG-H/L</b>	npDNA	CMV	CAG	TK	4018
6	npDNA-CAG-L		npDNA	CMV	CAG	TK	3331
7	<b>npDNA-CMV1-HL</b>		npDNA	CMV	CMV	BGH	5027
8	<b>npDNA-CMV1-LH</b>		npDNA	CMV	CMV	BGH	5027
9	<b>npDNA-CMV1-L-CMV2-H</b>		npDNA	CMV/CMV-NF-κB	CMV	RGB/BGH	4799
10	<b>npDNA-CMV1-H-CMV2-L</b>		npDNA	CMV/CMV-NF-κB	CMV	RGB/BGH	4799
11	npDNA-CMV1-H	<b>npDNA-CMV1-H/L</b>	npDNA	CMV	CMV	BGH	3089
12	npDNA-CMV1-L		npDNA	CMV	CMV	BGH	2402
13	npDNA-CMV2-H	<b>npDNA-CMV2-H/L</b>	npDNA	CMV- NF-κB	CMV	BGH	2861
14	npDNA-CMV2-L		npDNA	CMV- NF-κB	CMV	BGH	2174
15	npDNA-CRM4-H	<b>npDNA-</b>	npDNA	sk-CRM4	DES	BGH	3660
16	npDNA-CRM4-L		npDNA	sk-CRM4	DES	BGH	2973

		<b>CRM4-H/L</b>					
17	npDNA-MCK-H	<b>npDNA-MCK-H/L</b>	npDNA	CK6	DES	BGH	3712
18	npDNA-MCK-L		npDNA	CK6	DES	BGH	3025
19	npDNA-MCKI-H	<b>npDNA-MCKI-H/L</b>	npDNA	CK6	DES (INR)	BGH	3708
20	npDNA-MCKI-L		npDNA	CK6	DES (INR)	BGH	3021

Abbreviations: DES (murine desmin), DES-INR (murine desmin + initiator sequence),<sup>26</sup>

polyA (polyadenylation signal), bp (basepairs), pDNA (plasmid DNA), npDNA (Nanoplasmid),

H (4D5 heavy chain), L (4D5 light chain), TK (thymidine kinase), BGH (bovine growth hormone), RGB ( $\beta$ -globin), NF- $\kappa$ B (nuclear factor kappa-light-chain-enhancer of activated

B cells), sk-CRM4 (cis-regulatory module),<sup>25</sup> CK6 (creatine kinase enhancer).<sup>26</sup>

A Plasmid setups in bold are used throughout the different experiments.

B CAG, CMV1 and CMV2 are ubiquitous and CRM4, MCK and MCKI are muscle-specific promoters.

C Dual plasmids are a combination of a heavy and light chain plasmid with an identical promoter denoted as 'H/L'.

D In a single plasmid, the order of H and L in the name represent their order on the plasmid shown in Figure 1.

## FIGURE LEGENDS

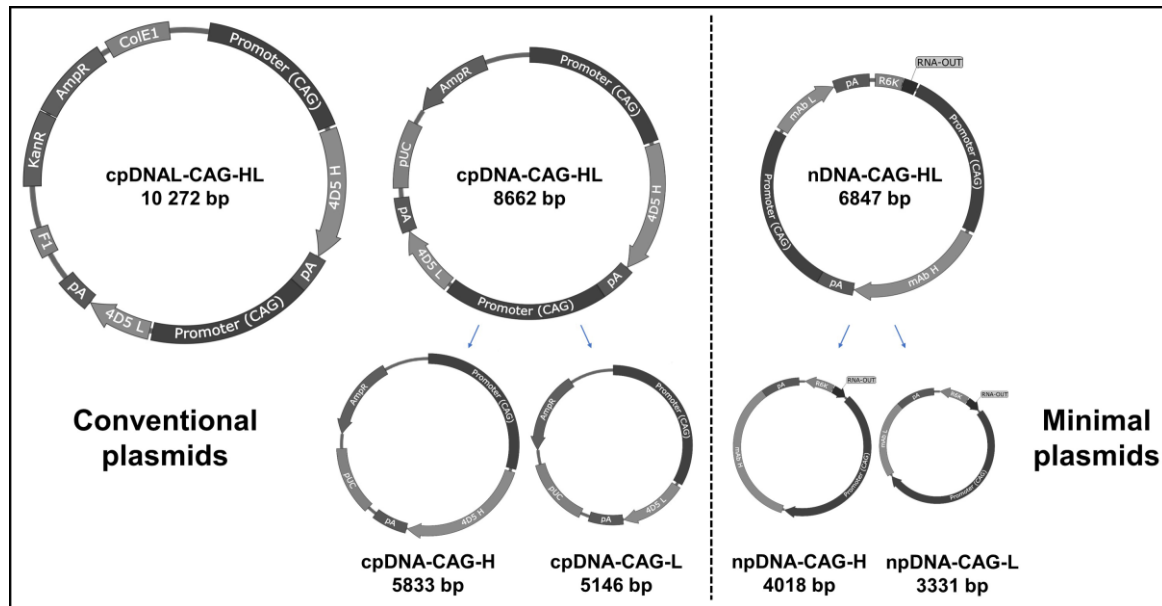


**Figure 1 | Overview of the evaluated single and dual plasmid backbones**

Single plasmid carrying 4D5 heavy and light chain expression cassettes (upper) or dual plasmids each carrying one expression cassette (lower) for the evaluated plasmid backbones, cpDNAL, cpDNA and npDNA. Promoter and polyadenylation (pA) elements of the expression cassette were variable (Table 1). AmpR (ampicillin resistance marker), KanR (kanamycin resistance marker), F1 (F1 ori), ColE1 (ColE1 Ori), pUC (pUC ori), R6K (R6K mini ori), L (light chain), H (heavy chain)



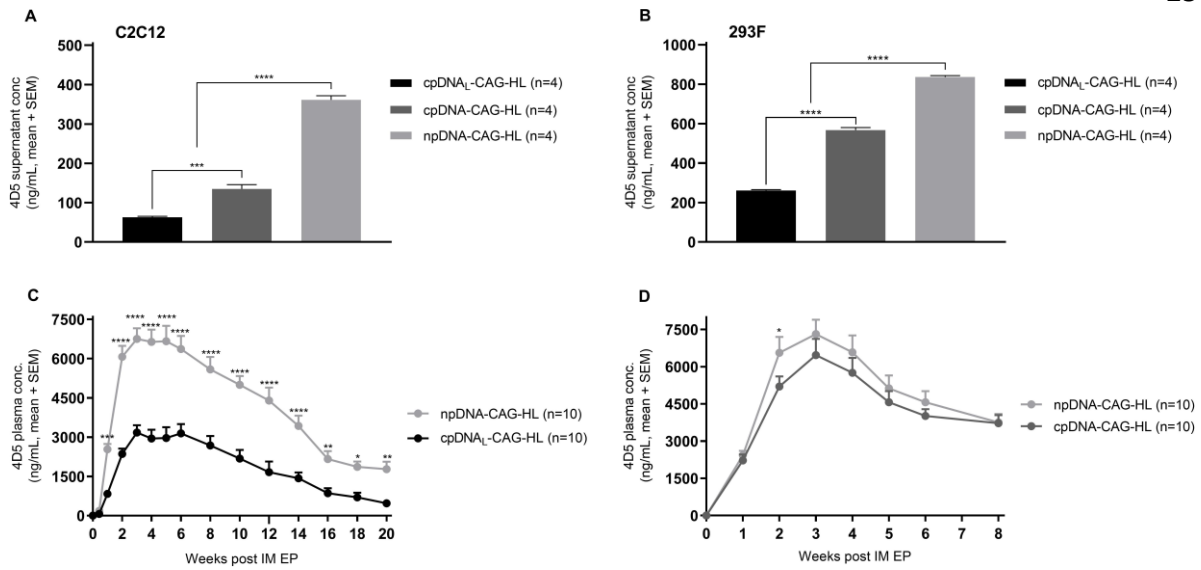


**Figure 2 | 4D5 levels after delivery of conventional and minimal plasmid backbones in vitro and in vivo**

4D5 supernatant levels six days after transfection in (A) C2C12 and (B) 293F for pDNA-CAG-HL and npDNA-CAG-HL. Pooled data from four experiments (n=4). 4D5 plasma levels over weeks post intramuscular (IM) electroporation (EP) of (C) 60 µg cpDNA<sub>L</sub>-CAG-HL and 40 µg npDNA-CAG-HL, (D) 50.4 µg cpDNA-CAG-HL and 40 µg npDNA-CAG-HL. Data are represented as mean + SEM. \* p ≤ 0.05; \*\* p ≤ 0.01; \*\*\* p ≤ 0.001; \*\*\*\* p ≤ 0.0001

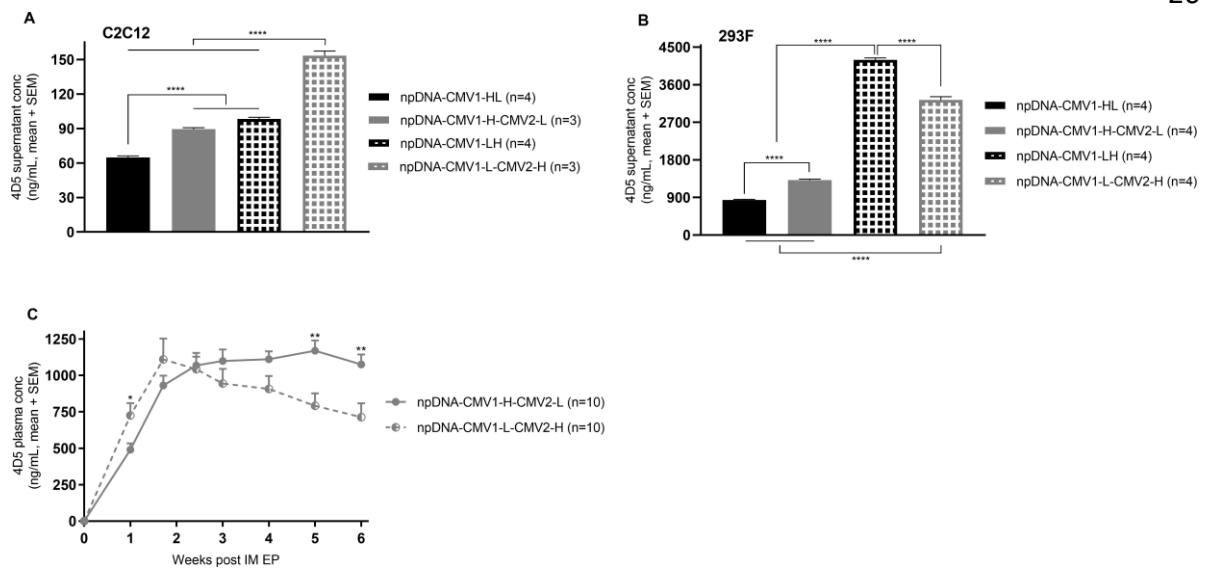


**Figure 3 | 4D5 levels after delivery of single plasmids with non-identical expression cassettes in vitro and in vivo**

4D5 supernatant levels six days after transfection in (A) C2C12 and (B) 293F for npDNA-CMV1-H-CMV2-L, npDNA-CMV1-L-CMV2-H, npDNA-CMV1-HL and npDNA-CMV1-LH.

Pooled data from four experiments (n=4) (C) 4D5 plasma levels over weeks post intramuscular (IM) electroporation (EP) of 60  $\mu$ g npDNA-CMV-H-CMV2-L and 60  $\mu$ g npDNA-CMV-L-CMV2-H. Data are represented as mean + SEM. \*  $p \leq 0.05$ ; \*\*  $p \leq 0.01$ ; \*\*\*\*  $p \leq 0.0001$

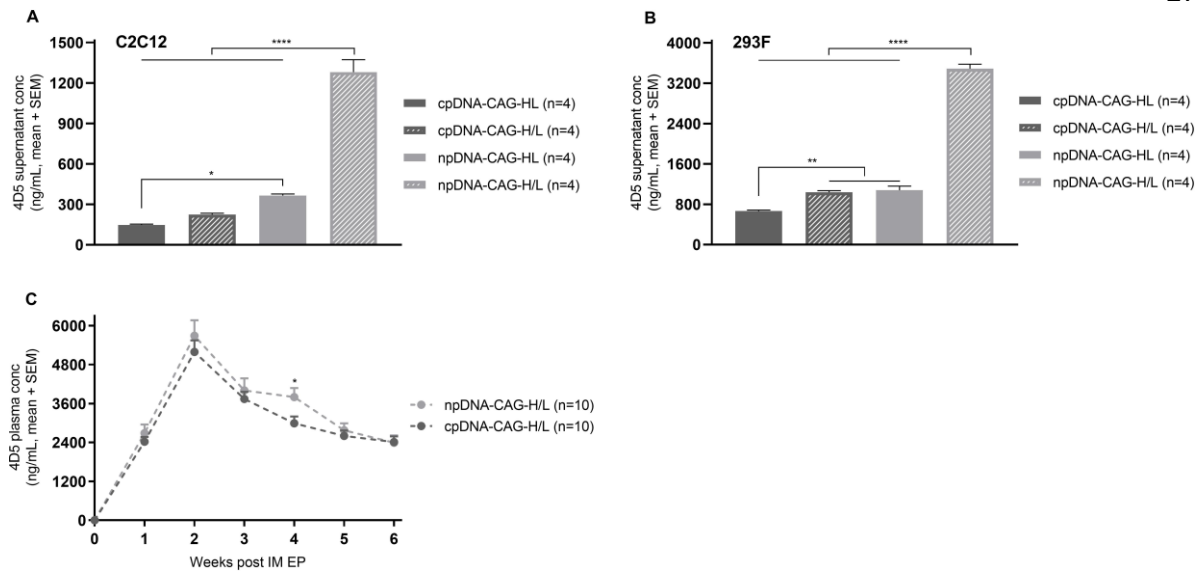


**Figure 4 | 4D5 levels after single or dual plasmid delivery**

4D5 supernatant levels six days after transfection in (A) C2C12 and (B) 293F for cpDNA-CAG-HL, cpDNA-CAG-H/L, npDNA-CAG-HL and npDNA-CAG-H/L. Pooled data from four experiments (n=4). (C) 4D5 plasma levels over weeks post intramuscular (IM) electroporation (EP) of 60  $\mu\text{g}$  cpDNA-CAG-H/L and 40.1  $\mu\text{g}$  npDNA-CAG-H/L. Data are represented as mean + SEM. \*  $p \leq 0.05$ ; \*\*  $p \leq 0.01$ ; \*\*\*\*  $p \leq 0.0001$

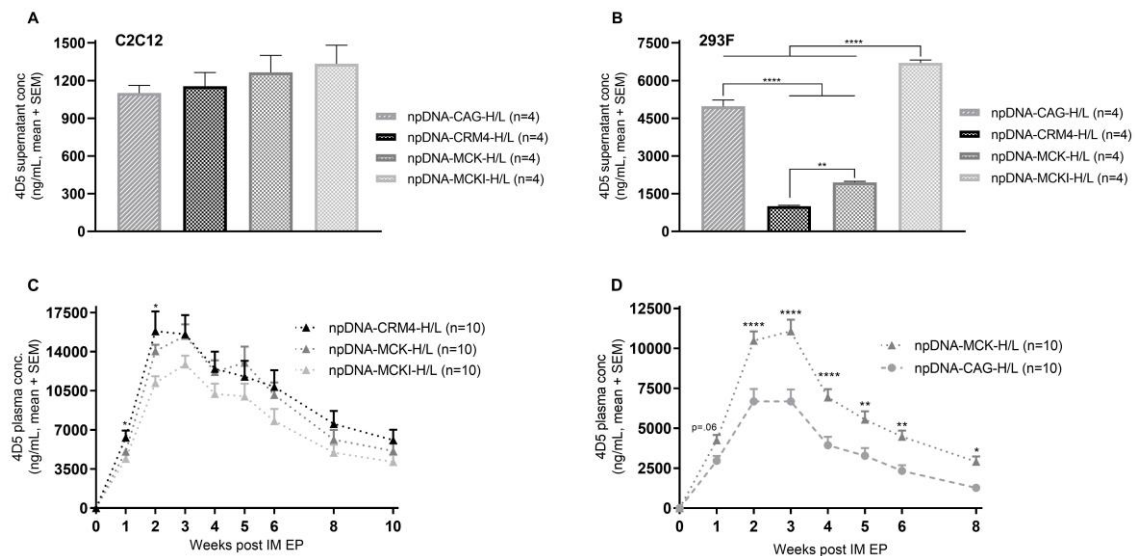


**Figure 5 | 4D5 levels after delivery of dual plasmids with ubiquitous and muscle-specific promoters in vitro and in vivo**

4D5 supernatant levels six after transfection in (A) C2C12 and (B) 293F for npDNA-CAG-H/L, npDNA-CRM4-H/L, npDNA-MCK-H/L and npDNA-MCKI-H/L. Pooled data from four experiments (n=4). 4D5 plasma levels over weeks post intramuscular (IM) electroporation (EP) of (C) 59  $\mu$ g npDNA-CRM4-H/L, 60  $\mu$ g npDNA-MCK-H/L and 60  $\mu$ g npDNA-MCKI-H/L; significant difference shown for npDNA-CRM4-H/L and npDNA-MCKI-H/L, (D) 60  $\mu$ g npDNA-CAG-H/L and 55  $\mu$ g npDNA-MCK-H/L. Data are represented as mean + SEM. \*  $p \leq 0.05$ ; \*\*  $p \leq 0.01$ ; \*\*\*  $p \leq 0.001$ ; \*\*\*\*  $p \leq 0.0001$